chrome P450s are natural fusion proteins (*15*), as are the mammalian nitric oxide synthases (*16*). In these examples, a monooxygenase activity is supported by reducing equivalents supplied by a reductase in the other domain. There is no requirement for redox cofactors in either the lipoxygenase or allene oxide reactions.

The allene oxide synthase domain of the coral protein has no sequence similarity to plant allene oxide synthases, which are hemoproteins of the cytochrome P450 superfamily (CYP74A) (*6*). The coral allene oxide synthase is also a hemoprotein, although it is related to catalase rather than the cytochrome P450 proteins. There are other examples of structurally unrelated proteins that mimic the type of chemistry associated with cytochrome P450s, including the chloroperoxidase of the mold *Caldariomyces fumago* (*17*) and the mammalian nitric oxide synthases (*18*). Both enzymes can catalyze P450-like reactions, an activity that has not been associated with catalase itself, possibly because of restricted access of substrates to the catalase active site (*12*, *19*). This active site topology limits the metabolism of alkyl peroxides and leaves the smaller hydrogen peroxide as the only natural substrate.

As regards mechanism, allene oxide synthesis is related to the formation of a wide array of products from fatty acid hydroperoxides. The initial steps of transformation involve a common intermediate (*20*), and thus the different reactions can be catalyzed by related enzymes. The coral allene oxide synthase may therefore be adapted to other catalytic activities. For example, starfish oocytes contain, in addition to 8*R*-lipoxygenase and allene oxide synthase, a hydroperoxide lyase that forms an aldehyde with 8*R*-HPETE as substrate (*21*). The synthesis of allene oxides may be but one manifestation of the catalytic activity of this fusion of lipoxygenase and catalase-related domains.

REFERENCES AND NOTES

1. A. J. Weinheimer and R. L. Spraggins, *Tetrahedron Lett.* (1969), p. 5185; A. J. Weinheimer, in *Prostaglandins from* Plexaura homomalla*: Ecology, Utilization and Conservation of a Major Medical Marine Resource*, F. M. Bayer and A. J. Weinheimer, Eds. (Univ. of Miami Press, Coral Gables, FL, 1974), pp. 17–21; G. L. Bundy, *Adv. Prostaglandin Thromboxane Leukotriene Res.* **14**, 229 (1985).
2. M. Hamberg, *J. Am. Oil Chem. Soc.* **66**, 1445 (1989); A. R. Brash, *J. Am. Chem. Soc.* **111**, 1891 (1989).
3. E. J. Corey, S. P. T. Matsuda, R. Nagata, M. B. Cleaver, *Tetrahedron Lett.* **29**, 2555 (1988); H. Kikuchi, Y. Tsukitani, K. Iguchi, Y. Yamada, *ibid.* **23**, 5171 (1982); B. J. Baker, R. K. Okuda, P. T. K. Yu, P. J. Scheuer, *J. Am. Chem. Soc.* **107**, 2976 (1985).
4. A. R. Brash, S. W. Baertschi, C. D. Ingram, T. M. Harris, *J. Biol. Chem.* **262**, 15829 (1987).
5. M. Hamberg and H. W. Gardner, *Biochim. Biophys. Acta* **1165**, 1 (1992).
6. W.-C. Song and A. R. Brash, *Science* **253**, 781 (1991); W.-C. Song, C. D. Funk, A. R. Brash, *Proc. Natl. Acad. Sci. U.S.A.* **90**, 8519 (1993).
7. A. R. Brash, W. E. Boeglin, M. S. Chang, B.-H. Shieh, *J. Biol. Chem.* **271**, 20949 (1996).
8. For the first round of PCR, we used cDNA from *P. homomalla* total RNA and the primers 5′-GGTTCCAARTGGYTNATGGCNAA and 5′-CTATGTRTGIATRCTRTTIGGIAT (*7*). For the second round of PCR, we used the equivalent of 0.1 μl of the first-round PCR products as template with the same upstream primer and the nested downstream primer 5′-CCAGATCAGIAAICCRTCRTCICKRTA. The 405-bp product included sequences from the previously identified 8*R*-lipoxygenase (*7*) and the lipoxygenase described here.
9. The 5′ end of the sequence was cloned with the Marathon cDNA Amplification kit (Clontech) (*7*) and the 5′ RACE procedure (Gibco-BRL).
10. J. C. Boyington, B. J. Gaffney, L. M. Amzel, *Science* **260**, 1482 (1993); W. Minor *et al.*, *Biochemistry* **35**, 10687 (1996).
11. C. D. Funk, *Prog. Nucleic Acid Res. Mol. Biol.* **45**, 67 (1993).
12. I. Fita and M. G. Rossman, *J. Mol. Biol.* **185**, 21 (1985).
13. The NH_2-terminal domain [amino acids 1 to 373 of the coding sequence, with or without a COOH-terminal $(His)_4$ tag] was expressed in the pET3a vector in *Escherichia coli* (BL21, Novagen) incubated at 28°C in TB medium for 24 hours. This resulted in appearance in the bacterial cytosolic fraction of a hemoprotein detectable by UV-visible spectroscopy (≈1 absorbance unit at 406 nm) that was not present in cells transfected with vector alone. The enzyme was purified by ammonium sulfate precipitation (30 to 55% fraction) and by anion exchange chromatography on Q-Sepharose, and on a nickel affinity column (Qiagen) for the His-tagged protein.
14. The lipoxygenase domain was expressed after deletion of the NH_2-terminus from the 5′ end to nucleotide 1116 of the ORF.
15. J. A. Peterson and S. E. Graham-Lorence, in *Cytochrome P450*, P. R. Ortiz de Montellano, Ed. (Plenum, New York, 1995), pp. 151–180.
16. Y. Wang and P. A. Marsden, *Adv. Pharmacol.* **34**, 71 (1995).
17. B. W. Griffin, in *Peroxidases in Chemistry and Biology*, J. Everse, K. E. Everse, M. B. Grisham, Eds. (CRC, Boca Raton, FL, 1991), pp. 85–137.
18. M. A. Marletta, *Cell* **78**, 927 (1994).
19. M. R. N. Murthy, T. J. Reid III, A. Sicignano, N. Tanaka, M. G. Rossman, *J. Mol. Biol.* **152**, 465 (1981); B. K. Vainshtein, W. R. Melik-Adamyan, V. V. Barynin, A. A. Vagin, A. I. Grebenko, *Nature* **293**, 411 (1981).
20. L. Crombie and D. O. Morgan, *J. Chem. Soc. Perkin Trans.* **1**, 581 (1991); W. H. Gerwick, *Lipids* **31**, 1215 (1996); M. Hamberg, *Acta Chem. Scand.* **50**, 219 (1996).
21. A. R. Brash *et al.*, *J. Biol. Chem.* **266**, 22926 (1991).
22. J. Steczko, G. A. Donoho, J. E. Dixon, T. Sugimoto, B, Axelrod, *Protein Expr. Purif.* **2**, 221 (1991); H. Ohta, Y. Shirano, K. Tanaka, Y. Morita, D. Shibata, *Eur. J. Biochem.* **206**, 331 (1992).

23. We thank W. Boeglin for help with the HPLC analyses and J. Swanson and his colleagues at the Keys Marine Laboratory for collection of the *P. homomalla* specimens. Supported by a grant from NIH (GM49502) and a Fogerty International Research Collaboration Award (TW00404).

30 May 1997; accepted 20 August 1997

Human DNA–(Cytosine-5) Methyltransferase–PCNA Complex as a Target for p21^{WAF1}

Linda S.-H. Chuang, Hang-In Ian, Tong-Wey Koh, Huck-Hui Ng, Guoliang Xu,* Benjamin F. L. Li†

DNA–(cytosine-5) methyltransferase (MCMT) methylates newly replicated mammalian DNA, but the factors regulating this activity are unknown. Here, MCMT is shown to bind proliferating cell nuclear antigen (PCNA), an auxiliary factor for DNA replication and repair. Binding of PCNA requires amino acids 163 to 174 of MCMT, occurs in intact cells at foci of newly replicated DNA, and does not alter MCMT activity. A peptide derived from the cell cycle regulator p21^{WAF1} can disrupt the MCMT-PCNA interaction, which suggests that p21^{WAF1} may regulate methylation by blocking access of MCMT to PCNA. MCMT and p21^{WAF1} may be linked in a regulatory pathway, because the extents of their expression are inversely related in both SV40-transformed and nontransformed cells.

DNA methylation in mammals is involved in imprinting (*1*), regulation of transcription (*2*), and development (*3*). Various diseases, including cancer (*4*) and fragile X syndrome (*5*), are associated with abnormal DNA methylation, which indicates that one or more regulatory mechanisms must exist to ensure the maintenance of precise methylation patterns by MCMT in the mammalian genome.

To investigate whether PCNA, an auxiliary factor for DNA replication and repair, was involved in the regulation of MCMT activity, we first determined whether the two proteins interact in vitro. We incubated human acute lymphoblastic leukemia (CEM) cell extracts with immobilized glutathione-S-transferase (GST) fusion proteins containing fragments of MCMT (Fig. 1, A and B) and analyzed the bound cellular proteins on immunoblots. Results with both cellular and recombinant PCNA (rPCNA, Fig. 1C) indicated that MCMT binds to PCNA directly through amino acids 122 to 322. We refer to this region as hMPBD (human methylase-PCNA binding domain). Further deletion analysis (Fig. 2, A to C) revealed that hMPBD requires only the sequence TRQTTITSHFAKG (*6*). Comparative studies on vertebrate MPBDs, as well as point-mutation analyses (Fig. 2, D to F), indicated that Arg^{163}, Gln^{164}, Thr^{166}, Ile^{167},

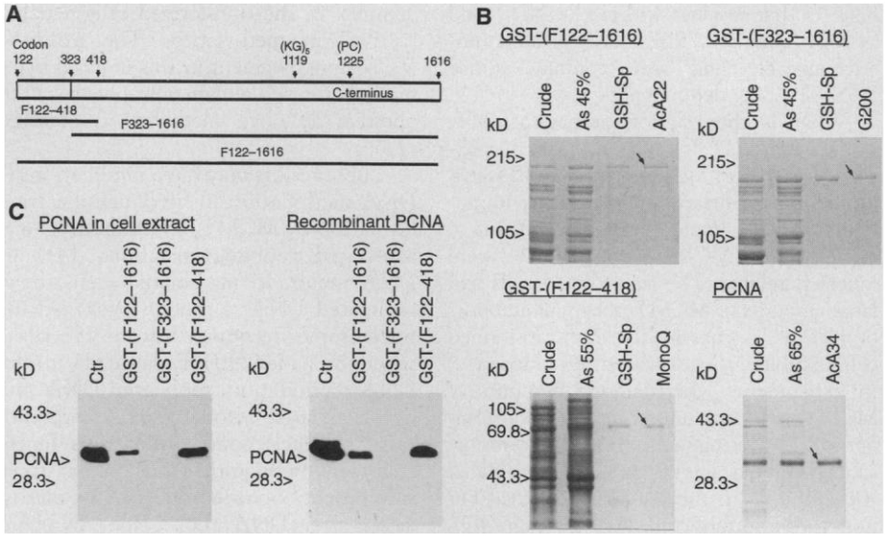

Fig. 1. Binding of PCNA to human recombinant MCMTs. (**A**) Map of the MCMT fragments used to construct GST fusion proteins. $(KG)_5$, hinge region; PC, active site; fragments (F) are labeled by the start and end codons. (**B**) SDS–polyacrylamide gel electrophoresis (SDS-PAGE) of fusion proteins detected by Coomassie staining (*23*). Lanes labeled "crude" contain bacterial lysates; As %, ammonium sulfate precipitates; GSH-Sp, GSH-Sepharose–purified fusion proteins; and MonoQ, the 0.1 M NaCl fraction from MonoQ (HR5/5) chromatography. AcA22, G200, and AcA34 are the gel filtration fractions. (**C**) Immunoblot of bound PCNA (*24, 25*). CEM cell extracts (200 μg) or rPCNA (100 ng) were incubated with 100 ng of GST-(F122–1616), GST-(F323–1616), or GST-(F122–418). The GST fusion proteins were recovered by GSH-Sepharose and the bound PCNA was detected by PCNA antibodies (PC10, 0.5 μg/ml). Ctr, control input PCNA.

His^{170}, and Phe^{171} are critical for binding to PCNA.

To test whether PCNA binding affected the nuclear localization of MCMT, we transfected SV40-transformed MRC5 cells (MRC5SV) with an expression vector encoding GST fused to codons 122 to 207 of MCMT (which includes both MPBD and the nuclear localization signal) and treated the cells with bromodeoxyuridine (BrdU) to label replicated DNA. In transfected cells costained with a polyclonal antibody to GST (anti-GST) and a monoclonal antibody (mAb) to BrdU, there was precise colocalization of the GST fusion protein with the newly incorporated BrdU in small nuclear speckles (Fig. 3, A, E, and I). By contrast, these fine speckles, which represent early replication foci, were not stained by anti-GST in cells transfected with the H170V null PCNA-binding mutant (Fig. 3, B, F, and J). Similar results were obtained with anti-GST and PCNA mAb (Fig. 3). The binding of PCNA does not alter the ability of MCMT to methylate poly(deoxyinosine-deoxycytidine) [poly(dI-dC)] substrates (Fig. 4A). Thus, PCNA binding to MCMT may recruit this DNA modification enzyme to methylate newly replicated DNA. Another replication foci–targeting domain has been mapped to codons 325 to 573 of murine MCMT; however, this sequence targeted the protein to "larger" or late replication foci (*7*).

The hMPBD motif resembles a sequence in the tumor suppressor $p21^{WAF1}$. This sequence (KRRQTSMTDFYHSKRRLIFS, corresponding to codons 141 to 160 of $p21^{WAF1}$) binds tightly to PCNA and inhibits the in vitro replication of SV40 DNA (*8*). We therefore compared the ability of the synthetic peptides corresponding to wtWPBD (wild-type $p21^{WAF1}$-PCNA binding domain), wtMPBD, and a chimeric MPBD-WPBD (Fig. 4B) to disrupt the MPBD-PCNA interaction. Less rPCNA bound to immobilized GST-MPBD after pretreatment of rPCNA with wtWPBD relative to pretreatment with wtMPBD (Fig. 4B). Similar results were observed when the wtWPBD and wtMPBD peptides were added to preformed GST-MPBD and PCNA complex (Fig. 4B). Because the chimeric peptide failed to compete, this result

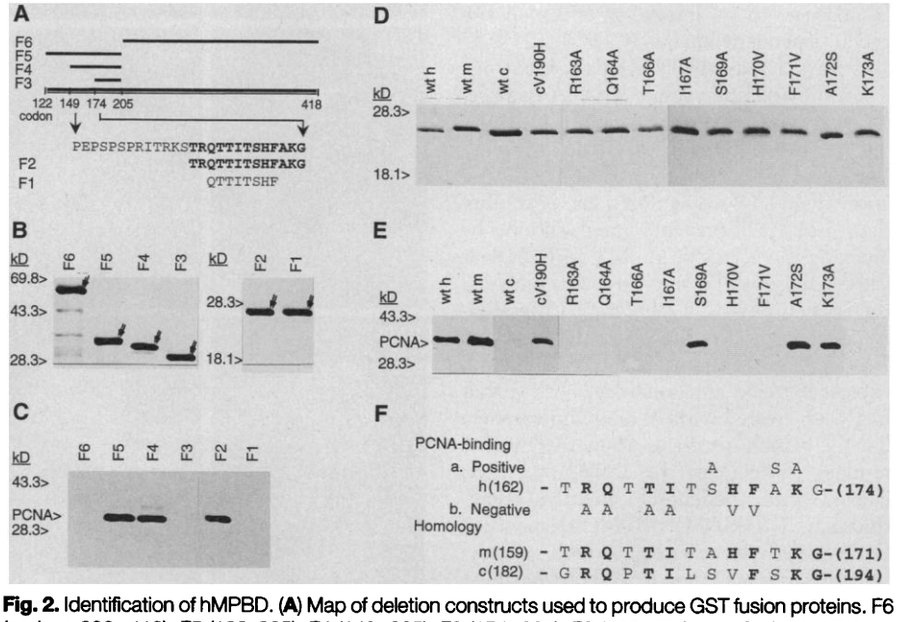

Fig. 2. Identification of hMPBD. (**A**) Map of deletion constructs used to produce GST fusion proteins. F6 (codons 206–418), F5 (122–205), F4 (149–205), F3 (174–205), F2 (162–174), and F1 (164–171) are fragments of F122–418 (*6, 23*). (**B**) SDS-PAGE of fusion proteins detected by Coomassie staining (*23*). (**C**) Immunoblot of bound PCNA (*24, 25*). rPCNA (100 ng) was incubated with the GSH-Sepharose–immobilized proteins in (B). (**D**) SDS-PAGE of vertebrate GST-MPBD derivatives by Coomassie staining [wt h, wt m, and wt c are wild-type human, murine, and chicken MPBDs, respectively; cV190H is a Val^{190} → His substitution at codon 190 of cMPBD, whereas others are human MPBD mutants (*6, 23*)]. (**E**) Immunoblot of PCNA bound to the samples in (D). (**F**) Schematic showing the PCNA-binding properties of human MPDB derivatives from (E). Residues that are critical for PCNA binding (except K173) and conserved in the m (mouse) and c (chicken) MPBDs are in bold (*6*).

L. S.-H. Chuang, H.-I. Ian, T.-W. Koh, H.-H. Ng, B. F. L. Li, Chemical Carcinogenesis Laboratory, Institute of Molecular and Cell Biology, National University of Singapore, Kent Ridge Crescent, Singapore 119260, Republic of Singapore.
G. Xu, Bioscience Centre, National University of Singapore, Kent Ridge Crescent, Singapore 119260, Republic of Singapore.
*Present address: Department of Genetics and Development, Columbia University, Hammer 1124, 701 West 168th Street, New York, NY 10032, USA.
†To whom correspondence should be addressed. E-mail: mcblib@leonis.nus.sg

suggests that residues within the NH_2- and COOH-terminiofWPBDandMPBDarenoninterchangeable and may contain unique PCNA-binding determinants.

What is the relation among MCMT, PCNA, and $p21^{WAF1}$ in intact cells? Surprisingly, analysis of asynchronous SV40-transformed and nontransformed cells by immunoblot (Fig. 4C) revealed that the extents of expression of MCMT and $p21^{WAF1}$ were inversely related. The transformed cells had large amounts of MCMT but small amounts of $p21^{WAF1}$, whereas the nontransformed cells exhibited the reverse pattern. However, in experiments where similar amounts of MCMT were immunoprecipitated for comparison (by using an excess of nontransformed cell extracts), PCNA coprecipitated with MCMT in the SV40-transformed but not the nontransformed cells (Fig. 4D). These results agree with the in vitro observation that WPBD can disrupt the MPBD-PCNA complex and suggest that $p21^{WAF1}$ may regulate the formation of the MCMT-PCNA complex in vivo. In addition, during the G_1-S transition, there must be one or more mechanisms that facilitate MCMT-PCNA interaction in the nontransformed cells.

Because MCMT preferentially methylates certain types of damaged DNA (9), the enzyme must be prevented from contacting damaged DNA sites in order to avoid unscheduled hypermethylation of the genome. In addition to its inhibitory effect on the cyclin-dependent kinases (CDKs), $p21^{WAF1}$ also plays a role in DNA repair. Upon induction by p53 as a result of DNA damage, $p21^{WAF1}$ colocalizes with PCNA at DNA repair sites (*10*). Because the MCMT-PCNA complex is fully active in methylation (Fig. 4A), we explored the possibility that $p21^{WAF1}$ prevents methylation by blocking the access of MCMT to PCNA at the repair sites. To test this, we compared the concentrations of [^{3}H]5meC (5-methyl-2′-deoxycytidine) formed in the genomic DNA of MRC5 and MRC5SV cells (which express extreme amounts of $p21^{WAF1}$) that had been treated with *N*-methylnitrosourea [NMU, which produces O^6-methylguanine residues (6MeG) in the DNA] and then labeled with S-adenosyl-L-[methyl-^{3}H]methionine ([^{3}H]SAM). O^6-Methylguanine–DNA methyltransferase, which repairs 6MeG, was inactivated by O^6-benzylguanine treatment before NMU addition (*11*). Consistently, the incorporated [^{3}H]5meC concentrations were found to be higher in the NMU-treated than in the untreated MRC5SV cells, but the opposite was observed for MRC5 cells (Fig. 4E). Thus, during DNA damage, the $p21^{WAF1}$ in the nontransformed cells appeared to "delay" methylation, whereas the stable MCMT-PCNA complex in the transformed cells remained "active" in methylation. The extent of MCMT involvement in this induced hypermethylation will remain unresolved until the putative de novo methylase is identified (*12*).

These results may have implications for DNA methylation in vivo, cellular transformation by MCMT, DNA methylation–associated genomic instability (*4*), and DNA repair. In mammalian cells, newly replicated DNA is rapidly packaged into nucleosomes to which histone H1 is subsequently added (*13*). Because H1 inhibits DNA methylation, replicated DNA must be methylated before H1 is incorporated into the nucleosomes (*13*). This limited time window requires a mechanism to ensure proper coordination of DNA methylation after DNA replication. PCNA is structurally similar to the β subunit of the *Escherichia coli* DNA polymerase complex, which can remain bound to the replicated DNA during its switch from polymerase III to the loader-unloader γ subunit (*14*). If PCNA behaves similarly to the β subunit in maintaining its association with the replicated DNA, then these PCNA molecules are potential sites for the loading of MCMT onto the replicated DNA. To accommodate the size of this replicated DNA or to prevent its interference with replication, MCMT may use a second replication foci–targeting domain B1 (downstream of MPBD, residues 325 to 573) (*7*) that can bind to replicated DNA of a particular size (*15*). With MPBD and B1 contacting the replicated DNA, the large domain between this region and the active site (the PC dipeptide) could "scan" for the hemimethylated sites for methylation.

Our data suggest that $p21^{WAF1}$ and

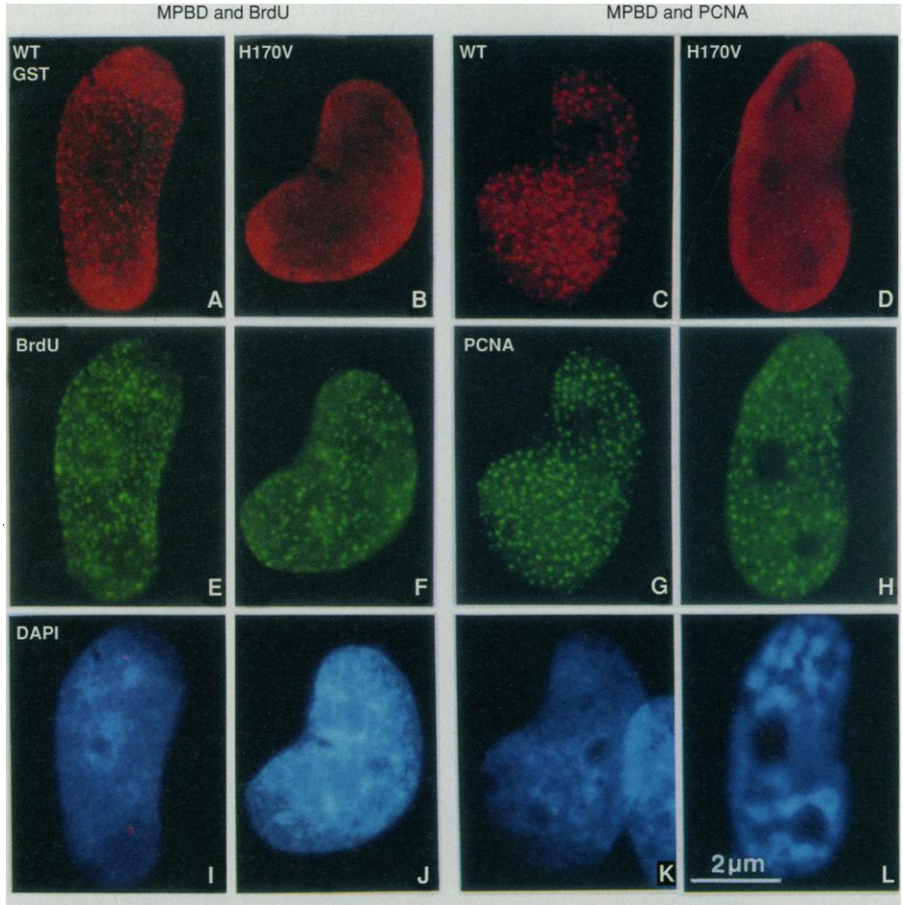

Codon 122 207
WT = GST–RQTTITSHFAKG–NLS–
H170V = GST–RQTTITSVFAKG–NLS–

Fig. 3. Colocalization of MPBD and PCNA with newly replicated DNA. MRC5SV cells were transfected with the GST fusion constructs of wild-type (WT) and H170V mutant inserts in pXJ41neo vector for 24 hours (*26*) and labeled with BrdU for 20 min. After fixation, cells were stained sequentially with anti-GST (10 μg/ml, for the expressed GST fusion proteins) and BrdU mAb (5 μg/ml) or anti-GST and PCNA mAb (PC10, 10 μg/ml) (*24, 26*). Left panels, colocalization of MPBD and BrdU (which represents newly replicated DNA); right panels, colocalization of MPBD and PCNA. Nuclear DNA is stained with 4,6-diamidino-2-phenylindole (DAPI). NLS, nuclear localization signal.

MCMT are potential antagonists. The quaternary $p21^{WAF1}$-PCNA–cyclin D1–CDK4 complex, which regulates G_1-S transition of the cell cycle, is stable in normal cell extracts but not in some virus-transformed and tumor cells (*16*). The cell-transforming activity of overexpressed MCMT and the high MCMT activities often present in tumor cells (*17*) suggest that MCMT may exert its oncogenic effects by competing with cellular $p21^{WAF1}$ for PCNA and may thereby perturb the stability of the quaternary complex. The released cyclin D1–CDK4 complex would phosphorylate and inactivate the retinoblastoma protein (Rb), a G_1 restriction point regulator, to stimulate cell proliferation (*16*). This might explain why the two SV40-transformed cells used in this study grow faster than their nontransformed counterparts (*18*).

The MCMT-PCNA interaction adds complexity to our understanding of DNA repair in vivo, because both nucleotide excision repair and mismatch repair require PCNA (*19*). However, by its presence at the DNA repair sites, $p21^{WAF1}$ may sequester the damaged DNA for repair and prevent hypermethylation, because it may inhibit MCMT from contacting PCNA while allowing DNA repair to continue (*20*). If this model is correct, the genomic instability observed in p53-deficient cells that cannot transactivate $p21^{WAF1}$ after DNA damage (*21*) may, in part, be attributable to aberrant methylation patterns in the genome, a characteristic of tumor cells (*4*).

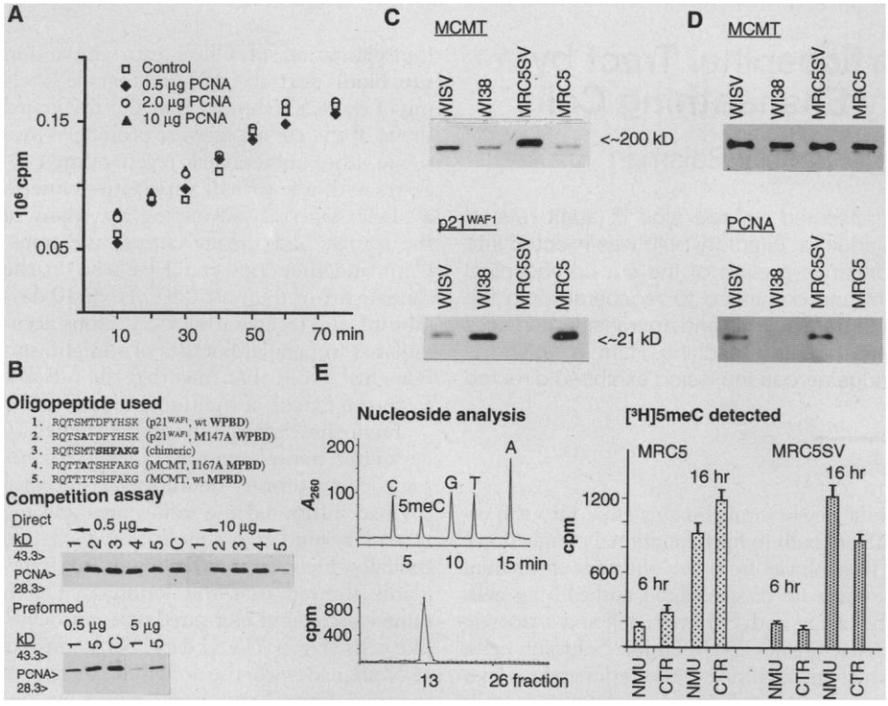

Fig. 4. Relation among MCMT, $p21^{WAF1}$, and PCNA. (**A**) Effect of PCNA on MCMT methylase activity. GST-(F122–1616) (7 μg) was incubated with rPCNA (0.5, 2, or 10 μg), poly(dI-dC) (2 μg), and [^{3}H]SAM (2 μM, 71 Ci/mmol) in assay buffer (*27*). The graph summarizes the average of two experiments and shows the time course of [^{3}H]CH_3 group incorporation into poly(dI-dC). (**B**) Comparative effect of MPBD and WPBD on binding of GST-MPBD to rPCNA (*25*). Top panel is the sequence of the peptide used (*6*). Peptide 2 is the null PCNA binding mutant of wtWPBD (*8*). In the competition assays, peptides were added to the rPCNA before binding by GST-MPBD proteins (direct) or added to the immobilized GST-MPBD and rPCNA complexes (preformed). The PCNA associated with GST-MPBD was analyzed by immunoblot. C indicates input rPCNA. (**C**) Immunoblot showing the amount of MCMT and $p21^{WAF1}$ present in the lysates [200 μg (*24*)] of SV40-transformed (MRC5SV and WISV) and nontransformed (MRC5 and WI38) cells. Blots were developed with mAb D12 (1 μg/ml) for MCMT and mAb Cip1 (1 μg/ml) for $p21^{WAF1}$. (**D**) Immunoblot of PCNA coprecipitated with MCMT from the cell lysates in (C) by anti-MCMT. To balance the small amounts of MCMT present in the nontransformed cell lysates [see (C)], 10-fold excesses of their immunoprecipitates were used for comparison with the SV40-transformed counterparts (*24*). Top, MCMT detected by mAb D12; bottom, coprecipitated PCNA (by PC10). (**E**) [^{3}H]5meC in the genomic DNA from NMU-treated and untreated (CTR) cells labeled with [^{3}H]SAM (*28*). Top left, a chromatogram of standard 2′-deoxynucleosides resolved by reversed-phase HPLC; bottom left, a control experiment where [^{3}H]5meC is detected by scintillation counting of the HPLC fractions from nucleoside analysis of poly(dI-dC) treated with GST-(F122–1616) and [^{3}H]SAM. The bar graph shows the relative amount of [^{3}H]5meC found in the genomic DNAs from NMU-treated and untreated MRC5 and MRC5SV cells, which were labeled with [^{3}H]SAM for 6 or 16 hours.

REFERENCES AND NOTES

1. E. Li, C. Beard, R. Jaenisch, *Nature* **366**, 362 (1993).
2. X. Nan, F. J. Campoy, A. Bird, *Cell* **88**, 471 (1997).
3. E. Li, T. H. Bestor, R. Jaenisch, *ibid.* **69**, 915 (1992).
4. S. B. Baylin *et al.*, *Cancer Cells* **3**, 383 (1991); J. L. Counts and J. I. Goodman, *Cell* **83**, 13 (1995); P. A. Jones, *Cancer Res.* **56**, 2463 (1996); C. Lengauer, K. W. Kinzler, B. Vogelstein, *Proc. Natl. Acad. Sci. U.S.A.* **94**, 2545 (1997).
5. S. T. Warrent and C. T. Ashley Jr., *Annu. Rev. Neurosci.* **18**, 77 (1995).
6. Abbreviations for the amino acid residues are as follows: A, Ala; C, Cys; D, Asp; E, Glu; F, Phe; G, Gly; H, His; I, Ile; K, Lys; L, Leu; M, Met; N, Asn; P, Pro; Q, Gln; R, Arg; S, Ser; T, Thr; V, Val; W, Trp; and Y, Tyr.
7. H. Leonhardt, A. W. Page, H. U. Weier, T. H. Bestor, *Cell* **71**, 865 (1992).
8. Y. Q. Chen, S. C. Cipriano, J. M. Arenkiel, F. R. Miller, *Cancer Res.* **55**, 4536 (1995); E. Warbrick, D. P. Lane, D. M. Glover, L. S. Cox, *Curr. Biol.* **5**, 275 (1995); J. M. Gulbis *et al.*, *Cell* **87**, 297 (1996).
9. N. W. Tan and B. F. L. Li, *Biochemistry* **29**, 9234 (1990).
10. L. Toschi and R. Bravo, *J. Cell Biol.* **107**, 1623 (1988); R. Li, G. J. Hannon, D. Beach, B. Stillman, *Curr. Biol.* **6**, 189 (1996).
11. H. K. Oh *et al.*, *Biochemistry* **35**, 12259 (1996).
12. H. Lei *et al.*, *Development* **122**, 3195 (1996).
13. T. Krude, *Curr. Biol.* **5**, 1232 (1995); R. Gasser, T. Koller, J. M. Sogo, *J. Mol. Biol.* **258**, 224 (1996); D. Carotti, S. Funiciello, P. Lavia, P. Caiafa, R. Strom, *Biochemistry* **35**, 11660 (1996); M. McArthur and J. O. Thomas, *EMBO J.* **15**, 1705 (1996).
14. X.-P. Kong, R. Onrust, M. O'Donnell, J. Kuriyan, *Cell* **69**, 425 (1992); T. S. R. Krishna, X.-P. Kong, S. Gary, P. M. Burgers, J. Kuriyan, *ibid.* **79**, 1233 (1994); D. R. Herendeen and T. J. Kelly, *ibid.* **84**, 5 (1996); V. Naktinis, J. Turner, M. O'Donnell, *ibid.*, p. 137.
15. L. S.-H. Chuang, H.-H. Ng, J. N. Chia, B. F. L. Li, *J. Mol. Biol.* **257**, 935 (1996).
16. Y. Xiong, H. Zhang, D. Beach, *Genes Dev.* **7**, 1572 (1993); S. R. Peterson, D. M. Gadbois, E. M. Bradbury, P. M. Kraemer, *Cancer Res.* **55**, 4651 (1995); Y. Xiong *et al.*, *J. Virol.* **70**, 999 (1996).
17. J. Wu *et al.*, *Proc. Natl. Acad. Sci. U.S.A.* **90**, 8891 (1993); T. L. Kautiainen and P. A. Jones, *J. Biol. Chem.* **261**, 1594 (1986); J. P. Issa *et al.*, *J. Natl. Cancer Inst.* **85**, 1235 (1993).
18. A. K. C. Teo and B. F. L. Li, unpublished data.
19. M. K. Shivji, M. K. Kenny, R. D. Wood, *Cell* **69**, 367 (1992); A. Nichols and A. Sancar, *Nucleic Acids Res.* **20**, 2441 (1992); A. Umar *et al.*, *Cell* **87**, 65 (1996).
20. M. K. Shivji, S. J. Grey, U. P. Strausfeld, R. D. Wood, J. J. Blow, *Curr. Biol.* **4**, 1062 (1994); S. Waga, G. J. Hannon, D. Beach, B. Stillman, *Nature* **369**, 574 (1994); Y. Luo, J. Hurwitz, J. Massague, *ibid.* **375**, 159 (1995).
21. W. S. El-Deiry *et al.*, *Cell* **75**, 817 (1993).
22. T.-C. Ayi, K.-C. Loh, R. B. Ali, B. F. L. Li, *Cancer Res.* **52**, 6423 (1992); A. Lim and B. F. L. Li, *EMBO J.* **15**, 4050 (1996); J. Sambrook, E. F. Fritsch, T. Maniatis, *Molecular Cloning: A Laboratory Manual* (Cold Spring Harbor Laboratory Press, Cold Spring Harbor, NY, 1989).
23. The cloning and expression procedures were described previously for F122–1616 and F323–1616 fragments (F) of MCMT (*15*). F122–418 in pGEX1was an Eco RI–Bst EII fragment. F6 in pGEX3 and F5 in pGEX1 were Mae II fragments of F122–418. F3 and F4 in pGEX2T were obtained with the polymerase chain reaction (PCR). F1, F2, and all vertebrate MPBD derivatives were cloned by oligonucleotide duplexes with Eco RI and Bam HI overhangs into pGEX2T (*15*). Human PCNA was cloned by PCR into pET3a. All sequences were confirmed by dideoxy sequencing. Proteins were induced with either 5 μM isopropyl-β-D-thiogalactoside (IPTG) for 48 hours at 22°C or 0.1 to 1 mM IPTG at 37°C for 3 hours. Proteins from bacterial lysates (*15*) were either purified on GSH-Sepharose or precipitated with ammonium sulfate before further purification.

24. For immunochemistry, cell extracts were prepared as described (*11*). Antibodies used are as follows: PC10 (anti-PCNA) from Santa Cruz; anti-GST, Protein-G$^{\gamma}$ purified rabbit antibodies raised against GST from pGEX2T; mAb D12 raised against GST-(F323–1616); anti-MCMT, GST-(F323–1616) affinity column–purified rabbit antibodies raised against GST-(F122–1616); mAb Cip1 (anti-p21^{WAF1}), from Transduction Lab. For immunoprecipitation, cell extract (2 mg) was incubated with anti-MCMT (13 μg) in IP buffer [equal volume of 50 mM tris (pH 7.5), 5% glycerol, and 0.2% Triton X-100] at 4°C for 1 hour. Protein G$^{\gamma}$–Sepharose (60 μl) beads were added for 2 hours. After washing three times with 500 μl of IP buffer (with 0.1 M NaCl), samples were boiled in Laemmli buffer for immunoblot.
25. For PCNA-binding, CEM cell extract (*11*) or rPCNA were added to binding buffer [100 μl, 50 mM tris (pH 7.5), 0.1% Triton X-100, 28 μM $ZnCl_2$, 10% glycerol, and 0.22 M KCl)] with GSH–Sepharose bead–bound fusion proteins. After shaking at 4°C for 40 min, the beads were recovered and washed three times with 500 μl of binding buffer before boiling in Laemmli buffer for immunoblot with PC10 antibody. In peptide competition assays, high-performance liquid chromatography (HPLC)–purified dodecapeptides (Research Genetics) were reconstituted to 2 mg/ml with argon-treated water and used directly.
26. For transient transfection assay (*22*), the WT GST-(F122–207) construct was obtained from F122–1616 by PCR and cloned into Not I–Kpn I sites of pXJ41neo. This was used for site-directed mutagenesis to create the H170V mutant (confirmed by dideoxy sequencing). After transfection, MRC5SV cells were labeled with BrdU (cell proliferation kit, Amersham) before staining (*7*, *22*).
27. Methylase activity assays were performed as described (*9*) but at 25°C with 10 min preincubation at 37°C. Aliquots (100 μl) were analyzed for tritiated poly(dI-dC) at 10-min intervals.
28. For [^{3}H]SAM labeling, cells in a 175-cm^2 (surface area) flask (75% confluent) were treated with O^6-benzylguanine [17 ml of 10 μM in serum-free media (SFM)] for 1 hour followed by addition of NMU (1 ml of 2.7 mM in SFM) or SFM with dimethyl sulfoxide as control (*11*). After 40 min, the media were removed and 11 ml of labeling mixture, containing 1.1 ml of dialyzed fetal bovine serum and 100 μCi of [^{3}H]SAM (75 Ci/mmol, Amersham) in amino acid–free modified Eagle's medium, was added for 6 or 16 hours. Genomic DNAs were isolated as described (*22*) and digested with venom phosphodiesterase (15 U) and shrimp alkaline phosphatase (10 U) in digestion buffer [25 mM tris (pH 8.0) with 2.5 mM Mg^{2+}, 300 μl per flask] for 16 hours at 37°C. The deoxynucleosides were analyzed by HPLC on a C-18 reversed-phase cartridge as described (*9*) and were quantified using standard 2′-deoxynucleosides (Sigma). [^{3}H]5meC was determined by scintillation counting of 0.5-ml fractions collected from each HPLC run and normalized to 1 mmol of total nucleosides detected. Two independent labeling experiments were performed.
29. We thank E. Manser for critical reading of the manuscript; Y. H. Tan and T. J. Lam for stimulating this collaboration; and R. B. Ali, A. Teo, and H. K. Oh for excellent assistance. Supported by the National Science and Technology Board of Singapore. This paper is dedicated to P. F. Swann (University College, London) for his constant encouragement to B.F.L.L.

1 May 1997; accepted 4 August 1997

Repair of Adult Rat Corticospinal Tract by Transplants of Olfactory Ensheathing Cells

Ying Li, Pauline M. Field, Geoffrey Raisman

The upper cervical corticospinal tract was transected on one side in adult rats. A suspension of ensheathing cells cultured from adult rat olfactory bulb was injected into the lesion site. This induced unbranched, elongative growth of the cut corticospinal axons. The axons grew through the transplant and continued to regenerate into the denervated caudal host tract. Rats with complete transections and no transplanted cells did not use the forepaw on the lesioned side for directed reaching. Rats in which the transplanted cells had formed a continuous bridge across the lesion exhibited directed forepaw reaching on the lesioned side.*

The failure of damaged nerve fibers to regenerate is the underlying cause of the permanent disabilities experienced by patients after spinal injury. Transplants of peripheral nerves (*1*) or Schwann cells cultured from peripheral nerves (*2*) have been used to induce reparative growth of axons in the adult rat central nervous system (CNS). The corticospinal tract (CST) is one of the main motor pathways of the spinal cord. After transection, the cut ends of the CST axons branch extensively but do not advance through the damaged area (*3*, *4*). Transplanted Schwann cells enhance the growth of cut CST axons, but there is little indication that the CST axons reenter host pathways (*3*, *5*).

Neurosensory cells of the adult olfactory system are continuously replaced (*6*), and their newly formed axons grow into the olfactory bulb to form functional connections. The pathway from the olfactory epithelium is made up of specialized ensheathing cells that share both Schwann cell and astrocytic characteristics (*7*–*9*). Unlike Schwann cells, which are confined to the peripheral nervous system, the olfactory ensheathing cells (OECs) accompany the olfactory axons into the CNS (*10*). We therefore examined whether injection of OECs cultured from adult olfactory bulb can improve the ability of regenerating CST axons to grow through a spinal cord lesion and reenter the host pathways.

OECs were obtained from the olfactory nerve and glomerular layers of syngeneic adult olfactory bulbs by the method of (*11*), but the final purification was omitted. Before transplantation the OECs were maintained in culture for 14 to 17 days. The cultures contained a variety of cell phenotypes (*8*). The CST was destroyed unilaterally by focal electrolytic lesions in the medioventral part of the dorsal columns between the first and second cervical segments (*3*, *12*) (Fig. 1). At 6 days after transplantation of OECs into the lesion site, biotin dextran (BD) anterograde labeling of the CST showed that the thickened shafts of the cut axons were prolonged into single, fine, unbranched, regenerating processes with a few small varicosities close to a single, tapering, advancing tip. Many of the sprouts had already crossed the transplant and their tips could be seen in the caudal part of the host CST. From 10 days onward, the regenerating CST axons accumulated in parallel bundles of straight, unbranched axons that traversed the full rostrocaudal extent of the transplants (Fig. 2).

From the earliest time point studied (6 days after transplantation), OECs expressing p75 low-affinity neurotrophin receptor (*8*) had infiltrated the lesion area and extended beyond it for at least 2 to 3 mm caudally. Electron microscopy of the transplants showed that the lesion area contained fascicles of elongated pale, astrocyte-like cells (Fig. 3A) and dark, Schwann-like cells aligned with the longitudinal axis of the tract. Over 2 to 3 weeks, the Schwann-like OECs established a one-to-one, peripheral-type myelinating relationship with individual CST axons, and the astrocyte-like OECs formed outer sheaths around groups of myelinated axons (Fig. 3B). After reentry into the caudal part of the host CST, the axons became myelinated by oligodendrocytes (Fig. 3C).

To explore whether these regenerating axons were capable of mediating useful function, we set up a pilot experiment to look for the presence or absence of a directed forepaw reaching function (DFR), in which the rats reach through an aperture to obtain a food reward (*13*). The rats were tested for one session a day on 10 successive days. During each session food pellets were presented until the rat had made 50 reaches through the aperture ("free" tests). For each

The Norman and Sadie Lee Research Centre, Division of Neurobiology, National Institute for Medical Research, Medical Research Council, London NW7 1AA, UK.

*This paper is dedicated to Diana, Princess of Wales, who inaugurated the Norman and Sadie Lee Research Centre in 1988. She gave years of unstinting support to people in wheelchairs. Her untimely death prevented her seeing this result, with which she would have been so pleased.